Circulation Research
Issue: Volume 106(3), 19 February 2010, pp 573-582

Publication Type: [Integrative Physiology]
DOI: 10.1161/CIRCRESAHA.109.204388
ISSN: 0009-7330
Accession: 00003012-201002190-00020
Keywords: familial dilated cardiomyopathy, lamin A/C, mechanical stress, exercise, carvedilol

Hide Cover

[Integrative Physiology]

Effects of Mechanical Stress and Carvedilol in Lamin A/C–Deficient Dilated Cardiomyopathy

Chandar, Suchitra*; Yeo, Li Sze*; Leimena, Christiana; Tan, Ju-Chiat; Xiao, Xiao-Hui; Nikolova-Krstevski, Vesna; Yasuoka, Yoshinori; Gardiner-Garden, Margaret; Wu, Jianxin; Kesteven, Scott; Karlsdotter, Lina; Natarajan, Shweta; Carlton, Arthur; Rainer, Stephen; Feneley, Michael P.; Fatkin, Diane

Author Information

From the Molecular Cardiology Division (S.C., L.S.Y., C.L., V.N.-K., Y.Y., J.W., L.K., S.N., D.F.) and Cardiac Physiology and Transplantation Division (J.-C.T., X.-H.X., S.K., M.P.F.), Victor Chang Cardiac Research Institute; Cancer Program (M.G.-G.), Garvan Institute of Medical Research; Synapse Technology Pty Ltd (A.C.); Division of Anatomical Pathology (S.R.) and Cardiology Department (M.P.F., D.F.), St Vincent's Hospital; and Faculties of Medicine and Life Sciences (M.P.F., D.F.), University of New South Wales, Sydney, Australia.

Original received July 2, 2009; revision received November 30, 2009; accepted December 3, 2009.

*Both authors contributed equally to this work.

Correspondence to Diane Fatkin, Victor Chang Cardiac Research Institute, Lowy Packer Building, 405 Liverpool St, PO Box 699, Darlinghurst NSW 2010, Australia. E-mail d.fatkin@victorchang.edu.au

Abstract

Rationale: Mutations in the *LMNA* gene, which encodes the nuclear lamina proteins lamin A and lamin C, are the most common cause of familial dilated cardiomyopathy (DCM). Mechanical stress-induced apoptosis has been proposed as the mechanism underpinning DCM in lamin A/C-deficient hearts, but supporting in vivo evidence has been lacking.

Objective: Our aim was to study interventions to modify mechanical stress in heterozygous *Lmna* knockout ($Lmna^{+/-}$) mice.

Methods and Results: Cardiac structure and function were evaluated before and after exercise training, thoracic aortic constriction, and carvedilol treatment. $Lmna^{+/-}$ mice develop adult-onset DCM with relatively more severe disease in males. $Lmna^{+/-}$ cardiomyocytes show altered nuclear morphology and perinuclear desmin organization, with enhanced responses to hypo-osmotic stress indicative of cytoskeletal instability. Despite these structural defects that provide a template for mechanical stress-induced damage, young $Lmna^{+/-}$ mice subjected to 6 weeks of moderate or strenuous exercise training did not show induction of apoptosis or accelerated DCM. In contrast, regular moderate exercise attenuated DCM development in male $Lmna^{+/-}$ mice. Sustained pressure overload generated by thoracic aortic constriction depressed ventricular contraction in young wild-type and $Lmna^{+/-}$ mice with no sex or genotype differences in the time-course or severity of response. Treatment of male $Lmna^{+/-}$ mice from 12 to 40 weeks with the [beta]-blocker, carvedilol, prevented the dilatation and contractile dysfunction that was observed in placebo-treated mice.

Conclusions: These data suggest that factors other than mechanical stress-induced apoptosis contribute to DCM and provide the first demonstration that regular moderate exercise and carvedilol can modify disease progression in lamin A/C-deficient hearts.

Mutations in the *LMNA* gene that encodes the nuclear lamina proteins lamin A and lamin C are the most common cause of familial dilated cardiomyopathy (DCM) identified to date,[1] accounting for 5% to 10% familial DCM overall and 30% to 45% families with DCM and conduction system disease (CD).[2–5] Affected individuals frequently have a rapidly progressive downhill clinical course, requiring pacemaker implantation or heart transplantation, with an increased risk of sudden death.[2–5] Despite the clinical importance of *LMNA* mutations, very little is known about mechanisms of disease pathogenesis and strategies to prevent DCM have not been investigated.

Because one-third of DCM-causing *LMNA* mutations are stop codons, splice site variants or insertions/deletions that reduce lamin A/C protein levels,[1,5] *Lmna* knockout mice are a useful and clinically relevant model to study DCM mechanisms.[6] We have previously reported that homozygous *Lmna* knockout ($Lmna^{-/-}$) mice exhibit severe DCM by 4 to 6 weeks.[7] Heterozygous *Lmna* knockout ($Lmna^{+/-}$) mice show CD at 10 weeks and DCM in later adult life.[8] A detailed analysis of the cardiac conduction-system in these mice has recently been performed.[8] The basis for DCM in $Lmna^{+/-}$ mice remains unexplained and is the major focus of this study.

Lamins are intermediate filament proteins present in the nuclear lamina and matrix that are critical determinants of nuclear architecture and function. A fundamental and unanswered question is how defects in these nuclear proteins cause cardiac contractile dysfunction. Cells lacking lamin A/C have altered nuclear shape and chromatin organization and show increased deformability and reduced viability in response to biaxial strain in vitro.[9,10] Because of these nuclear structural defects, it has been proposed that cardiomyocyte loss attributable to mechanical stress-induced apoptosis might be an important determinant of impaired contraction in lamin A/C–deficient hearts ("structural hypothesis").[11,12] Myocardial apoptosis is an attractive disease mechanism because it is seen in failing hearts and "wear-and-tear" effects of repeated cardiac contractions and hemodynamic load could account for age-related DCM in individuals with *LMNA* mutations. In addition to intrinsic nuclear defects, altered interactions between the nucleus and the cytoskeleton may further predispose to mechanical stress-induced damage. Desmin filaments form an intricate web that links myofibrils with the nucleus, intercalated discs and costameres. We found altered perinuclear desmin organization in $Lmna^{-/-}$ cardiomyocytes and proposed a model in which loss of nuclear anchoring attributable to lack of lamin A/C destabilizes the desmin scaffolding and promotes altered force transduction.[7] Despite the compelling rationale for the "structural hypothesis," in vivo data to validate mechanical stress as a determinant of DCM in lamin A/C–deficient hearts are lacking.

The central hypothesis underpinning our study is that interventions which increase mechanical stress will promote DCM and conversely, that reduction of mechanical stress will attenuate DCM in $Lmna^{+/-}$ mice. We first performed a detailed characterization of cardiac structure and function in male and female $Lmna^{+/-}$ mice. Although a trend toward a higher prevalence of *LMNA* mutations in females has been suggested,[4] the effects of sex on disease severity have not been evaluated. To determine the "wear and tear" effects of enhanced cardiac contractile activity, young wild-type (WT) and $Lmna^{+/-}$ mice without DCM were subjected to periods of moderate and strenuous exercise treadmill training. We hypothesized that exercise would induce apoptosis and accelerate the onset of DCM. We also evaluated the effects of thoracic aortic constriction (TAC) in WT and $Lmna^{+/-}$ mice. TAC is a widely used intervention to induce left ventricular (LV) pressure overload and is known to increase cardiomyocyte apoptosis.[13] We hypothesized that $Lmna^{+/-}$ mice would have increased apoptotic vulnerability and contractile impairment after TAC.

[beta]-Adrenergic receptor blocking drugs reduce myocardial chronotropic and inotropic activity and are widely used in the treatment of symptomatic heart failure.[14] Individuals with DCM caused by *LMNA* mutations are generally treated with standard heart failure therapies, including [beta]-blockers, once symptoms develop. Although genotype-positive family members can be identified preclinically, no preventative interventions have been studied. To determine whether [beta]-blocker therapy would mitigate against the development of DCM, we also evaluated the effects of carvedilol in young $Lmna^{+/-}$ mice. These data provide the first comprehensive in vivo analysis of mechanical stress in lamin A/C–deficient hearts and the first evaluation of therapeutic interventions to modify disease progression.

Methods

Animals

Lmna knockout mice in a C57Bl6×129Sv genetic background were generated as described.[6] Mice were genotyped by PCR amplification of tail DNA. Mutant mice and WT littermates were studied according to protocols approved by the institutional Animal Ethics Committee.

Cardiac Procedures

Echocardiography was performed as described.[7] Mice were ventilated and anesthetized for surgical procedures with ketamine (75 mg/kg), xylazine (20 mg/kg), and atropine (0.6 mg/kg). Heart rates were obtained using telemetry (Data Sciences International, Arden Hill, Minn) and were analyzed using AcqKnowledge version 3.1 software (Biopac Systems Inc, Goleta, Calif). TAC was achieved by placement of a ligature (6.0 silk) between the innominate and left common carotid arteries. Aortic pressure gradients were determined in anesthetized mice (isoflurane 1% to 3%) using 1.4F and 1.0F microtip catheter pressure transducers (Millar Instruments Inc, Houston, Tex).

Exercise Training

Exercise performance was assessed using an Eco 3/6 rodent treadmill (Columbus Instruments, Columbus, Ohio) and an exercise tolerance test comprised of graded increments of running speed (7 to 25 m/min) at 3-minute intervals with a fixed 5^0 incline. Exercise tolerance test end points were: final stage achieved and number of stimuli received from a grid at the base of each lane if running speed was not maintained. For moderate exercise training, mice ran at 17 m/min for 40 minutes at a 5^0 incline, 5 sessions/wk for 6 weeks.[15] For strenuous exercise training, mice ran at the highest tolerated speed (titrated from 15 m/min to 22 m/min over a 3-week period) for 40 minutes at a 15^0 incline, 2 sessions/wk for 6 weeks.[16] Each regimen included 2 days of acclimatization and 10 minutes of warm-up and cool-down periods.

Drug Studies

Carvedilol (Roche, Mannheim, Germany) was mixed with 1.5% Triton X-100 and administered at a dose of 10 mg/kg per day in drinking water.[17] Control mice received 1.5% Triton X-100 in drinking water.

Myocyte Studies

Cardiomyocyte morphology, shortening, and Ca^{2+} transients were evaluated as described.[7]

For osmotic studies, isolated cardiomyocytes were placed in basic Tyrode solution, then sequentially perfused at 37°C in isotonic (1T) and hypotonic (0.5T) solutions (80 mmol/L NaCl in basic Tyrode solution replaced with 160 mmol/L and 22.5 mmol/L mannitol, respectively), followed by a washout in 1T solution.[18] Myocyte images were captured (MyoCam; IonOptix Corp, Milton, Mass) and dimensions obtained using Image Tool software.

Histopathology

Sections (4 μm) of paraffin-embedded hearts stained with hematoxylin/eosin were examined using light microscopy. Frozen tissue sections were fixed then incubated with anti-desmin antibody (Ab) (1:100 dilution, Novocastra Laboratories Ltd, Newcastle, United Kingdom) and a fluorescein isothiocyanate–conjugated secondary Ab. DNA fragmentation detected by TUNEL assay [7] was quantified as the apoptotic index (number of TUNEL-positive nuclei divided by the total number of cardiomyocytes). To detect caspase activation, deparaffinized sections were rehydrated and incubated with cleaved caspase-3 Ab (1:200 dilution, Cell Signaling Technology Inc, Danvers, Mass) and a fluorescein isothiocyanate–conjugated secondary Ab. Sections were counterstained with DAPI and examined using fluorescence microscopy at ×40 magnification. Immunogold electron microscopy was performed as described.[7] The distribution of gold-labeled desmin in standardized regions of interest was evaluated quantitatively using nearest-neighbor analysis.[19]

Protein Analysis

Total protein extracts were separated by SDS-PAGE and hybridized with primary anti-desmin Ab (1:100 dilution, Novocastra) or total and phosphorylated anti-p44/42 MAPK Ab, anti–stress-activated protein kinase/c-Jun N-terminal kinase (anti-SAPK/JNK) Ab, anti-p38 MAPK Ab (all 1:1000 dilution, Cell Signaling); or anti-[beta]-actin Ab (1:400 dilution, Sigma-Aldrich, St Louis, Mo) with horseradish peroxidase–conjugated or Alexa Fluor 680/750 secondary Abs. Hybridization signals were quantified and normalized to [beta]-actin.

Statistical Analysis

Differences between groups were assessed using ANOVA and Student *t* test. Data are expressed as means±SD, and probability values of <0.05 were considered statistically significant.

Results

Cardiac Phenotype

Lmna$^{+/-}$ mice have slowly progressive DCM from 20 weeks with relatively more severe disease in males than females (Figure 1; Online Figure I and Table I in the Online Data Supplement, available at http://circres.ahajournals.org). Long-term survival was reduced in male and female *Lmna*$^{+/-}$ mice because of sudden death or heart failure necessitating euthanasia (Figure 1E). Overall myofibrillar architecture was normal in *Lmna*$^{+/-}$ hearts at all ages studied (Figure 2A and 2B, and data not shown), with patchy LV fibrosis seen in only 1 of 10 *Lmna*$^{+/-}$ mice evaluated at 80 weeks. *Lmna*$^{+/-}$ nuclei were characteristically longer and thinner than WT nuclei with irregular chromatin distribution and altered alignment (Figure 2B and 2D). Low levels of apoptosis were present in *Lmna*$^{+/-}$ hearts before and after the development of DCM with no age or genotype differences (Figure 1F). Isolated cardiomyocytes from male and female *Lmna*$^{+/-}$ mice aged 40 weeks showed normal morphology, shortening, and Ca^{2+} transients (Table 1).

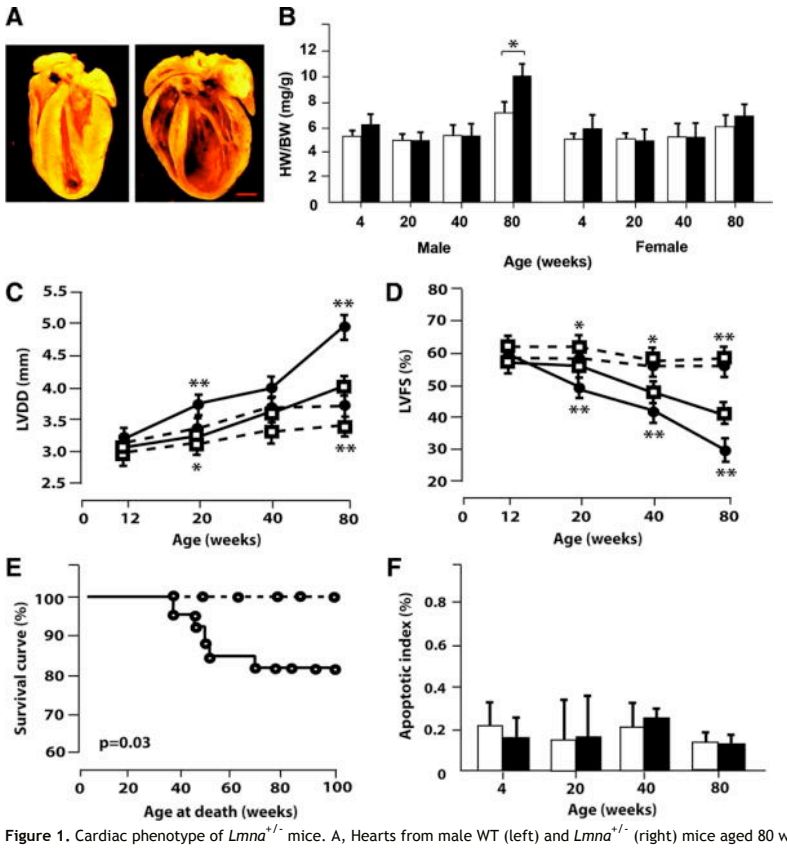

Figure 1. Cardiac phenotype of *Lmna*$^{+/-}$ mice. A, Hearts from male WT (left) and *Lmna*$^{+/-}$ (right) mice aged 80 weeks. Scale bar=2 mm. B, Heart weight (HW) to body weight (BW) ratios in male and female WT (n=6 to 12 each group, open bars) and *Lmna*$^{+/-}$ mice (n=6 to 20 each group, solid bars). Serial echocardiography from 12 to 80 weeks in male (solid circles) and female (open squares) WT (n=25, 10 male, dashed lines) and *Lmna*$^{+/-}$ mice (n=24, 14 male, solid lines). Changes in LVDD (C) and LVFS (D) are shown. E, Kaplan-Meier plot showing survival in WT (n=24, 10 male, dashed lines) and *Lmna*$^{+/-}$ mice (n=26, 16 male, solid lines). Five *Lmna*$^{+/-}$ mice (3 male) died suddenly, and 4 *Lmna*$^{+/-}$ mice (3 male) were euthanized for signs of heart failure. F, LV apoptosis in WT (n=5 to 17 each group, open bars) and *Lmna*$^{+/-}$ mice (n=6 to 17 each group, solid bars). *P<0.05, **P<0.01 (Student t test).

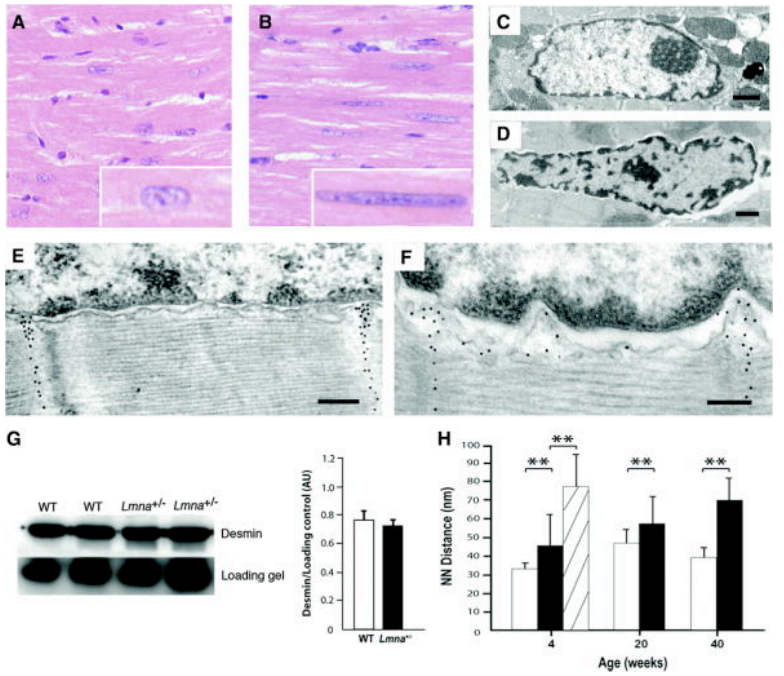

Figure 2. Myocardial histopathology in male 40-week-old mice. Sections stained with hematoxylin/eosin from WT (A) and *Lmna*$^{+/-}$ (B) mice showing differences in nuclear morphology (insets). Electron micrographs of cardiomyocyte nuclei in WT (C) and *Lmna*$^{+/-}$ (D) mice. Scale bar=1 μm. Immunogold electron microscopy demonstrates differences in the distribution of perinuclear gold-labeled desmin filaments (black dots) between WT (E) and *Lmna*$^{+/-}$ (F) cardiomyocytes. Scale bar=200 nm. G, Desmin protein levels in WT and *Lmna*$^{+/-}$ ventricles assessed by Western blotting, with bar graphs indicating mean protein levels. H, Distances between gold-labeled desmin epitopes in

regions of interest were quantified using nearest neighbor (NN) analysis. A minimum of 30 regions was randomly selected in images obtained from 2 to 3 mice of each age and genotype. Open bars indicate WT mice; solid bars, *Lmna*$^{+/-}$ mice; striped bars, *Lmna*$^{-/-}$ mice. *P<0.05, **P<0.01 (Student t test).

Table 1. Functional Studies of Ventricular Cardiomyocytes

	Male		Female	
	WT	*Lmna*$^{+/-}$	WT	*Lmna*$^{+/-}$
Myocyte length (μm)	121±10	126±8	118±8	122±5
Myocyte width (μm)	28±4	27±3	26±3	24±2
Sarcomere length (μm)	1.61±0.03	1.62±0.04	1.57±0.06	1.60±0.05
Shortening (%)	4.4±1.2	4.2±1.6	4.9±1.7	3.8±1.1
Time to peak shortening (ms)	67±8	66±16	65±5	60±7
Time to 50% relaxation (ms)	70±18	64±22	62±12	64±12
Baseline Ca^{2+} transient	0.80±0.07	0.78±0.08	NA	0.76±0.06
Peak transient amplitude	0.23±0.03	0.25±0.08	NA	0.24±0.04
Time to peak amplitude (ms)	48±10	41±8	NA	34±8
Time to 50% decay (ms)	120±38	144±29	NA	164±29

Ventricular cardiomyocytes (n=80–84 each group) were isolated from WT (n=17, 11 male) and *Lmna*$^{+/-}$ (n=17, 10 male) mice aged 40 weeks. Contractile function was assessed using edge detection. Cells were loaded with the Ca^{2+}-sensitive fluorescent dye Indo-1/AM, and intracellular [Ca^{2+}] was measured as the change in the 405:485 nm emission ratio. Values are reported as relative change in fluorescence ratio units following subtraction of background values. NA indicates not available.

Table 1. Functional Studies of Ventricular Cardiomyocytes

Desmin Organization and Osmotic Stress Responses

There was relative disorganization of perinuclear desmin in *Lmna*$^{+/-}$ cardiomyocytes that increased with age (Figure 2F and 2H). These desmin changes were not seen in another model of severe DCM caused by overexpression of a [beta]$_2$-adrenergic receptor transgene (Online Figure II).20 Desmin protein levels in *Lmna*$^{+/-}$ hearts were normal (Figure 2G). To investigate the functional consequences of these desmin changes, the dimensions of isolated cells from 12-week-old mice were assessed before and after exposure to a hypotonic bathing solution that induces cell swelling (Table 2). A 12-week “early” time point was selected to detect changes that precede DCM (Figure 1). At baseline, the length and width of WT and *Lmna*$^{+/-}$ cells were similar. In 0.5T solution, there were no changes in cell length but cell width increased in both groups. When compared with baseline data, the mean increment in cell width was relatively greater for *Lmna*$^{+/-}$ cells than WT cells. Osmotic studies were repeated in 40-week-old *Lmna*$^{+/-}$ mice that have established DCM (Figure 1) and disproportionate radial swelling was also seen (Table 2). Because desmin filaments are thought to be the predominant determinants of radial stability in cardiomyocytes,21 these findings are most readily explained by impaired desmin function.

Table 2. Osmotic Studies in Ventricular Cardiomyocytes

	12 Weeks		40 Weeks	
	WT	*Lmna*$^{+/-}$	WT	*Lmna*$^{+/-}$
No. cells	120	120	79	80
Baseline				
Length (μm)	122.3±11.4	120.7±7.3	137.4±6.0	141.9±4.3
Width (μm)	21.4±1.6	20.3±1.6	26.4±0.9	25.6±1.3
1T				
Length (μm)	121.8±12.3	120.1±8.2	132.0±9.0	137.6±9.1
Width (μm)	21.5±1.7	20.0±1.9	26.8±1.5	26.5±2.2
0.5T				
Length (μm)	124.1±13.1	122.9±8.9	133.8±8.3	138.9±8.6
Width (μm)	23.6±1.8	24.4±2.0	29.9±0.7	30.6±1.4
1T (washout)				
Length (μm)	121.9±12.1	120.4±8.4	128.9±12.8	133.0±13.0
Width (μm)	21.3±1.8	20.8±2.2	27.0±1.3	26.8±1.9
Change (baseline −0.5T)				
Length (%)	1.4±1.4	1.8±2.3	2.5±4.0	2.0±3.5
Width (%)	10.4±0.8	20.2±1.7*	13.4±1.6	19.8±0.7*

Ventricular cardiomyocytes were isolated from 12- and 40-week-old male WT and *Lmna*$^{+/-}$ mice (n=4–6 each group) and placed in basic Tyrode solution. Cell dimensions were measured at baseline and 8 minutes after sequential bathing in isotonic (1T) and hypotonic (0.5T) Tyrode solution. *$P<0.05$ vs WT (Student t test).

Table 2. Osmotic Studies in Ventricular Cardiomyocytes

Effects of Exercise Training

There were no differences in baseline exercise tolerance test or echocardiographic parameters in WT and *Lmna*$^{+/-}$ mice aged 12 weeks. After 6 weeks of moderate exercise training, exercise performance improved in both groups with an increase in the proportion of mice reaching the final stage of the exercise tolerance test and a reduction in the number of stimuli received (Online Table II). Cardiomyocyte nuclear morphology was qualitatively similar in sedentary and trained *Lmna*$^{+/-}$ hearts with no evidence of an exercise-induced increase in apoptosis, assessed by TUNEL assay or levels of activated caspase-3 (Figure 3A and Online Table III). LV end-diastolic diameter (LVDD) and fractional shortening (LVFS) were similar in trained and sedentary male WT mice. Trained male *Lmna*$^{+/-}$ mice had relatively higher LVDD and lower LVFS than trained WT mice. However, LV size and function in trained *Lmna*$^{+/-}$ mice were not significantly worse than in sedentary *Lmna*$^{+/-}$ mice (Figure 3C and 3E; Online Table II). When baseline and postexercise data were compared, trained male *Lmna*$^{+/-}$ mice had relatively *less* change in LVDD ([DELTA]LVDD) and LVFS ([DELTA]LVFS) than sedentary male *Lmna*$^{+/-}$ mice over the same time period. There were only small differences in LV size and between sedentary female WT and *Lmna*$^{+/-}$ mice, and these were unchanged by moderate exercise.

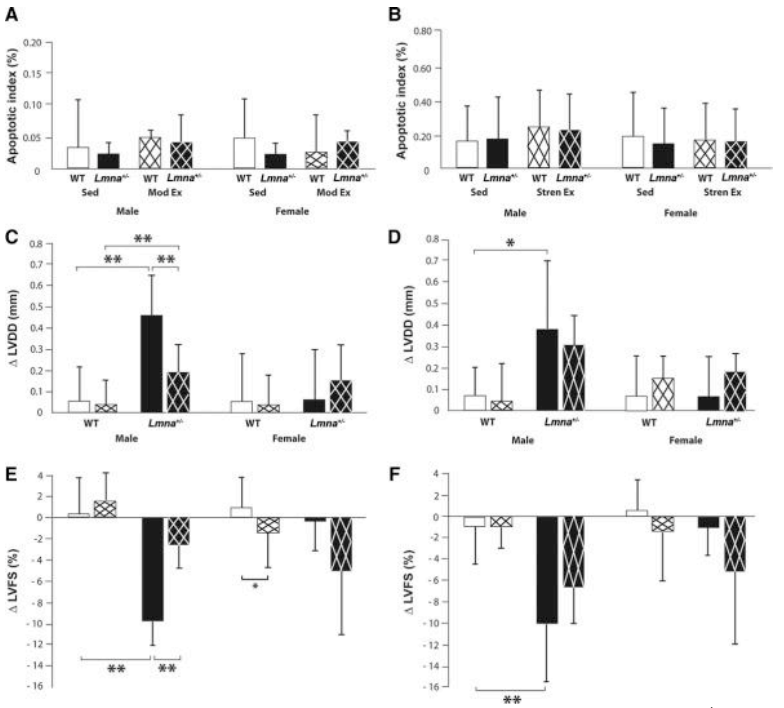

Figure 3. Effects of exercise. Apoptosis was assessed in 18-week-old male and female WT and *Lmna*$^{+/-}$ mice after 6 weeks of moderate (A) or strenuous (B) exercise training and was compared with age- and sex-matched sedentary mice. Echocardiography was performed before and after training. Changes in LVDD ([DELTA]LVDD) (C) and LVFS ([DELTA]LVFS) (E) after moderate exercise training in WT (n=23, 11 male,) and *Lmna*$^{+/-}$ (n=23, 13 male) mice were compared with age- and sex-matched sedentary WT (n=25, 10 male) and *Lmna*$^{+/-}$ (n=23, 14 male) mice. Open bars indicate sedentary WT mice; solid bars, sedentary *Lmna*$^{+/-}$ mice; cross-hatched bars, exercised mice. Effects of strenuous exercise training (D and F) in trained WT (n=12, 6 male) and *Lmna*$^{+/-}$ (n=12, 6 male) mice were compared with sedentary WT (n=31, 13 male) and *Lmna*$^{+/-}$ (n=32, 19 male) mice. *P<0.05, **P<0.01 (ANOVA and Student t test).

To determine the effects of exercise intensity, a separate cohort of mice underwent a regimen of twice-weekly strenuous exercise, in which the degree of difficulty was up-titrated to maximal tolerated levels at weekly intervals as peak performance improved. A similar exercise protocol exacerbates myocardial histopathology in *mdx* mice that lack the cytoskeletal protein, dystrophin.[16] This regimen proved to be initially more difficult for *Lmna*$^{+/-}$ mice; however, exercise performance improved with training (Online Table IV). There were no differences in apoptosis between sedentary and trained WT and *Lmna*$^{+/-}$ mice (Figure 3B and Online Table V). LVDD and LVFS in trained male and female *Lmna*$^{+/-}$ mice remained similar to sedentary mice (Figure 3D and 3F; Online Table IV). The beneficial effects of regular moderate-intensity exercise training on the [DELTA]LVDD and [DELTA]LVFS seen in male *Lmna*$^{+/-}$ mice were not recapitulated with the intermittent high-intensity exercise regimen.

Effects of TAC

TAC was performed in 12-week-old mice. All male mice developed myocardial hypertrophy with an increase in the heart weight/body weight ratio (Figure 4C). Male WT and *Lmna*$^{+/-}$ mice also showed LV dilatation and reduced contraction with no genotype differences at 7, 14 or 21 days post-TAC (Figure 4A and 4B; Online Table VI). Responses to TAC in female WT and *Lmna*$^{+/-}$ mice were similar to male mice (Figure 4A and 4B; Online Table VII).

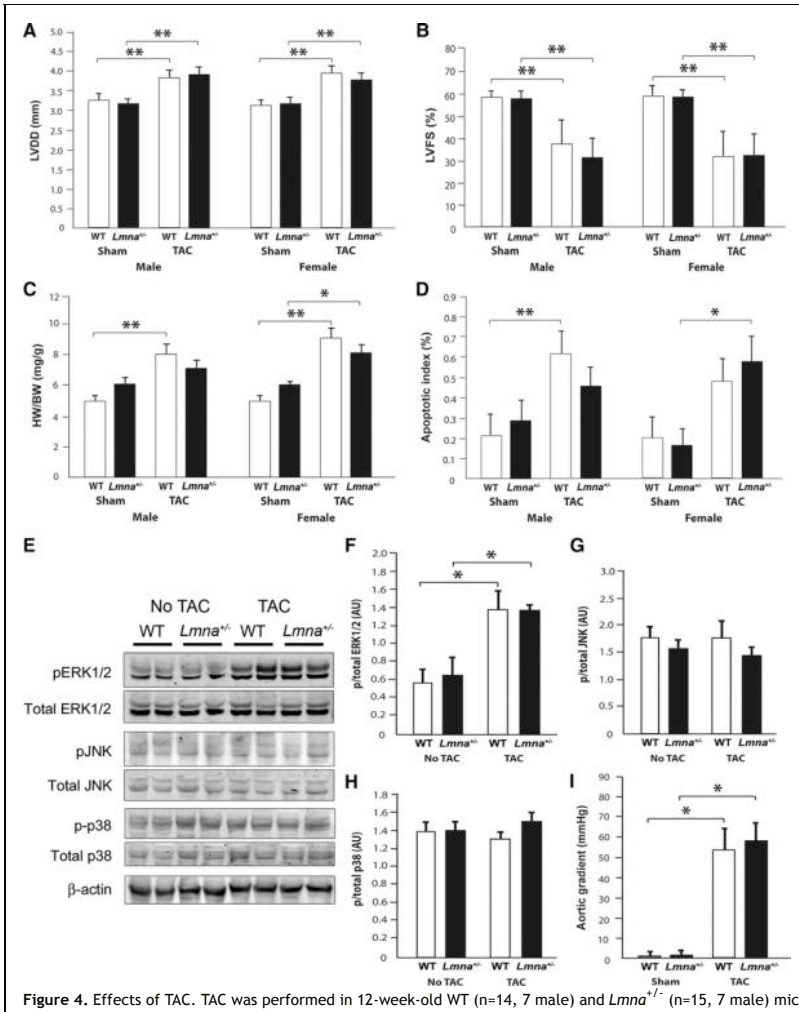

Figure 4. Effects of TAC. TAC was performed in 12-week-old WT (n=14, 7 male) and *Lmna*$^{+/-}$ (n=15, 7 male) mice. LVDD (A), LVFS (B), heart weight/body weight ratio (HW/BW) (C), and apoptosis (D) at 14 days post-TAC were compared with sham-operated WT (n=10, 5 male) and *Lmna*$^{+/-}$ (n=9, 5 male) mice. E through H, MAPK pathway activation was evaluated in male WT and *Lmna*$^{+/-}$ mice before and at 14 days after TAC. Levels of phosphorylated ERK1/2, JNK, and p38 were assessed after normalization to [beta]-actin and expressed as a ratio with total ERK1/2, JNK, and p38. Representative gels (E) and quantification of replicates (n=3) (F through H) are shown. I, Mean aortic gradients at 14 days in sham-operated and TAC mice. Open bars indicate WT mice; solid bars, *Lmna*$^{+/-}$ mice. *P<0.05, **P<0.01 (ANOVA and Student t test).

Mitogen-activated protein kinase (MAPK) signaling pathways regulate myocyte growth and survival in response to mechanical stress 22 and have recently been implicated in cardiac dysfunction in laminopathies.23 Western blot analysis showed increased levels of phosphorylated extracellular signal-regulated kinase (ERK)1/2 in LV tissue at 14 days after TAC, with no change in JNK or p38 proteins. There were no differences in indices of MAPK activation at baseline or after TAC between WT and *Lmna*$^{+/-}$ mice (Figure 4E through 4H). When compared with sham-operated mice, banded mice showed higher levels of apoptosis, but there were no differences in the apoptotic index or in levels of activated caspase-3 between banded WT and *Lmna*$^{+/-}$ mice (Figure 4D and Online Table VIII).

Effects of [beta]-Adrenergic Receptor Blockade

To determine whether early administration of [beta]-blocking drugs prevents DCM, carvedilol was administered in drinking water to male WT and *Lmna*$^{+/-}$ mice from 12 weeks. In placebo-treated *Lmna*$^{+/-}$ mice, LVDD increased and LVFS decreased with age. These changes were prevented by carvedilol, with no differences in LVDD or LVFS between active-treated *Lmna*$^{+/-}$ mice and WT mice at 40 weeks (Figure 5 and Online Table IX).

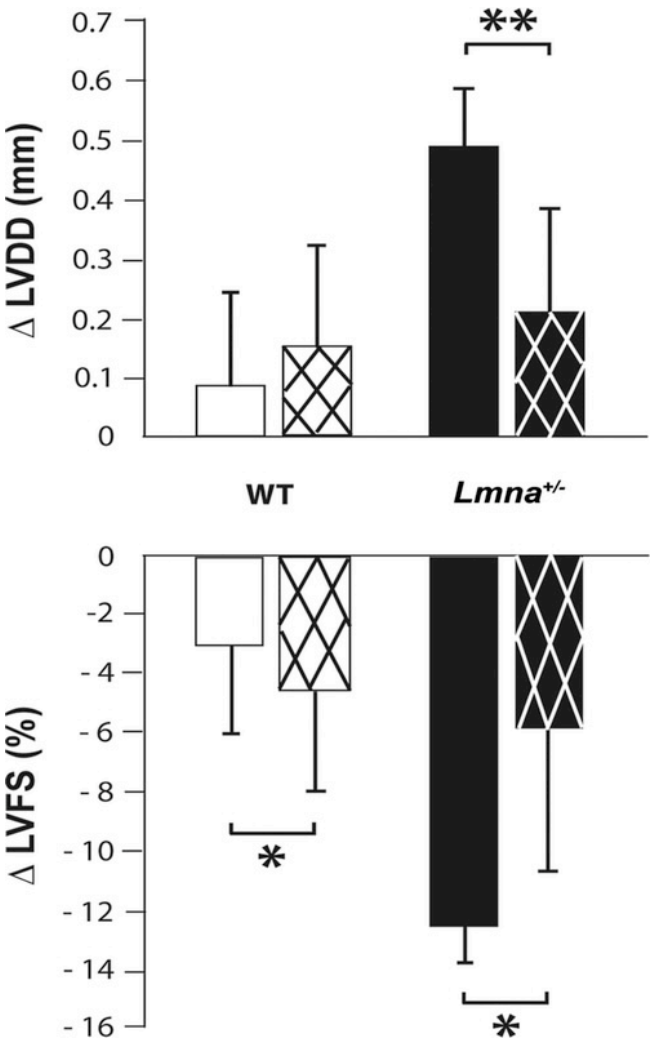

Figure 5. Effects of carvedilol. Echocardiography was performed in male WT (n=18) and *Lmna*$^{+/-}$ (n=17) mice before (12 weeks) and after (40 weeks) treatment with carvedilol or placebo. Changes in LVDD ([DELTA]LVDD) and LVFS ([DELTA]LVFS) were determined. Open bars indicate placebo-treated WT mice; solid bars, placebo-treated *Lmna*$^{+/-}$ mice; cross-hatched bars, carvedilol-treated mice. *P<0.05, **P<0.01 (ANOVA and Student t test).

Discussion

Here, we find that *Lmna*$^{+/-}$ mice develop adult-onset DCM with sex differences in disease severity. Despite cardiomyocyte nuclear and cytoskeletal abnormalities that could predispose to mechanical stress-induced damage, *Lmna*$^{+/-}$ mice did not have a predilection to develop apoptosis or contractile dysfunction in response to exercise or pressure overload. These data suggest that factors other than mechanical stress-induced apoptosis contribute to DCM in lamin A/C-deficient hearts.

Adult-Onset DCM in *Lmna*$^{+/-}$ Mice

Cardiac dysfunction is a prominent feature of *Lmna*$^{-/-}$ mice 7 and several transgenic mouse models of *LMNA* mutations.24–26 Our data confirm a recent report that *Lmna*$^{+/-}$ mice develop adult-onset DCM.8 Reduced shortening of isolated cardiomyocytes from old (50 to 75 weeks) *Lmna*$^{+/-}$ mice has been described 8 but this was not seen in cells from 40-week-old mice in this study. Varying experimental conditions, biological variability, and the absence of physiological loading conditions may contribute to these differences. Our data extend previous observations by additionally showing that males have a relatively greater severity of DCM than females. Sex differences in myocardial function have been described for a number of genetically modified mice and have been attributed both to multiple factors, including estrogens, estrogen receptors and diet.27 There are very little data about effects of sex in human laminopathies and further evaluation is required. In one series, there was a nonsignificant trend toward an increased prevalence of *LMNA* mutations in female familial DCM probands.4 Another longitudinal study in genotype-positive family members did not find sex to be a significant predictor of heart failure or ventricular arrhythmias.5

Nuclear and Cytoskeletal Structural Defects in *Lmna*$^{+/-}$ Mice

Embryonic fibroblasts from *Lmna*$^{+/-}$ mice have enhanced nuclear deformability with biaxial strain 10 and it can be inferred that dysmorphic *Lmna*$^{+/-}$ cardiomyocyte nuclei would have similar defects. *Lmna*$^{-/-}$ cardiomyocytes show marked disorganization of perinuclear desmin,7 and we now find similar but milder changes in *Lmna*$^{+/-}$ cardiomyocytes that precede DCM. The disproportionate increases in width of *Lmna*$^{+/-}$ cardiomyocytes when subjected to osmotic stress suggests that altered nuclear anchoring compromises the scaffolding function of desmin.21 Whether disruption of the nuclear connections of other cytoskeletal components, such as the spectrin repeat-containing nesprin and Sun proteins, contributes to these findings requires further evaluation.28 Intact physical connections between the nucleus and cytoskeleton are required for effective mechanotransduction in cells.7,29 Taken together, these data support a model in which altered nuclear-cytoskeletal coupling may reduce the efficiency of force transmission in cardiomyocytes with consequent impairment of contraction.

Exercise Training Does Not Induce Apoptosis or Accelerate DCM

To determine the effects of enhanced cardiac contractile activity, we used an exercise treadmill regimen that results in a moderate intensity of exercise, ie, O_2 consumption of [almost equal to]80% Vo_{max}, in mice.15 In contrast to our predictions, we found that moderate exercise training from 12 weeks of age did not induce apoptosis or accelerate the development of DCM in *Lmna*$^{+/-}$ mice. In fact, cardiac function in trained male *Lmna*$^{+/-}$ mice deteriorated to a lesser extent than occurred in age- and sex-matched sedentary *Lmna*$^{+/-}$ mice.

The “wear-and-tear” argument is based on the premise that mechanical stresses imposed on the myocardial wall during exercise have detrimental effects. Adaptive hemodynamic responses occur with training, including reductions of heart rate, contractility, and LV preload, that reduce net daily cardiac work and wall stress. Hence, to more stringently evaluate the role of mechanical stress, we subjected mice to a twice-weekly strenuous exercise regimen. LV size and function in trained *Lmna*$^{+/-}$ mice were similar to sedentary mice, indicating not only that the mechanical burden of the more demanding exercise protocol did not promote DCM but also that the benefits of the more frequent moderate exercise training regimen were not obtained. The possibility that different exercise treadmill regimens or different types of exercise could be detrimental to *Lmna*$^{+/-}$ mice cannot be excluded however.

Lmna$^{+/-}$ Mice Do Not Have Greater Susceptibility for Apoptosis or DCM After TAC

WT and *Lmna*$^{+/-}$ hearts responded to the sustained increase in LV afterload induced by TAC with myocardial hypertrophy, stress-induced MAPK activation, and depressed contraction. LV dysfunction is a recognized complication of TAC that has been attributed primarily to cell loss and fibrosis.13 Although we predicted that TAC would have exaggerated effects in *Lmna*$^{+/-}$ mice, neither the severity of LV functional impairment nor the degree of apoptosis was relatively greater than that observed in WT littermates up to 21 days post-TAC.

Apoptosis in Other Lamin A/C–Related DCM Models

Mice overexpressing N195K and M371K *Lmna*, respectively, develop DCM in adult life but do not have significant levels of LV apoptosis under baseline conditions.25,26 Young (4-week-old) *Lmna*$^{+/-}$ mice lack LV free wall apoptosis but do show CD and apoptosis in atrioventricular node cells.8 Taken together, these observations indicate that myocardial apoptosis is unlikely to be a primary cause of DCM in any of these models, and further suggest that CD and LV dysfunction can occur as independent pathologies.

Exercise and Carvedilol Favorably Modify Disease Progression

Exercise training at moderate intensity improves peak oxygen consumption increases exercise time and improves quality of life in patients with heart failure.30 These benefits have been attributed to factors such as reduced resting heart rate and blood pressure, increased coronary blood flow, improved vascular endothelial function, reduced platelet aggregation, reduced oxidative stress, improved lipid and blood glucose levels, and modification of obesity and mental stress.30 Although it is generally assumed that exercise in heart failure is beneficial, studies in murine models suggest that the effects may vary according to the cause of DCM. For example, cytoskeletal protein models such as desmin-null, dysferlin-null, and dystrophin-deficient *mdx* mice, have a worse outcome with exercise.16,31,32

Carvedilol also has negative inotropic and chronotropic actions, as well as potent vasodilation, antiischemic, antiapoptotic and antioxidant effects.33 Given that mechanical stress-induced apoptosis does not explain lamin A/C–related DCM, it seems likely that the hemodynamic and antiapoptotic benefits of exercise and carvedilol are relatively less important than other direct myocardial effects. Antioxidant actions of exercise and carvedilol are of particular interest in view of recent data implicating oxidative stress in heart failure and in other laminopathy phenotypes, including lipodystrophy, premature ageing, and amyotrophic quadricipital syndrome with cardiac involvement.34,35 Further studies of the role of oxidative stress and changes induced by exercise training and carvedilol in *Lmna*$^{+/-}$ hearts are warranted.

Clinical Implications

Because individuals at risk of DCM can be recognized early by genetic testing or by presentation with CD, identification of preventive strategies is imperative. The “structural hypothesis” predicts that enhanced cardiac contractile activity would accelerate DCM in patients with *LMNA* mutations and thus exercise should be avoided. Although our study was designed to determine the role of mechanical stress as a primary pathogenic factor, potential adverse effects once DCM is manifest cannot be excluded. Genotype-positive individuals who engage in high level

competitive sport for prolonged periods (10 years or longer) have recently been shown to have a 3- to 4-fold increased risk of adverse cardiac events.5 Although the numbers were relatively small, these data urge caution in exercise recommendations to families. An exciting finding in young male *Lmna*$^{+/-}$ mice was that regular moderate exercise and carvedilol appeared to protect against DCM development. Whether these benefits are also seen in older female mice and patients with established DCM will be important to ascertain.

Acknowledgments

We thank Colin L. Stewart for providing the *Lmna* knockout mice and Xiao-Jun Du for [beta]$_2$-adrenergic receptor transgenic mice. We also thank Mark Hicks for pharmacological supplies; Matt Wand for statistical advice; Robert Graham and Peter Macdonald for helpful discussions; and Aisling McMahon, Jan Michalicek, and Ishtiaq Ahmed for assistance with physiological studies.

Sources of Funding

This work was supported by the National Health and Medical Research Council of Australia, the Sylvia and Charles Viertel Charitable Foundation, and the Cardiac Society of Australia and New Zealand.

Disclosures

None.

References

Non-standard Abbreviations and Acronyms	
Ab	antibody
CD	conduction system disease
DCM	dilated cardiomyopathy
ERK	extracellular signal-regulated kinase
LV	left ventricular
LVDD	left ventricular end-diastolic diameter
LVFS	left ventricular fractional shortening
MAPK	mitogen-activated protein kinase
TAC	thoracic aortic constriction
WT	wild type

Table. **Non-standard Abbreviations and Acronyms**

1.Fatkin D, Otway R, Richmond Z. Genetics of dilated cardiomyopathy. *Heart Fail Clin*. In press. [Context Link]

2.Fatkin D, MacRae C, Sasaki T, Wolff MR, Porcu M, Frenneaux M, Atherton J, Vidaillet HJ, Spudich S, De Girolami U, Seidman JG, Seidman CE. Missense mutations in the rod domain of the lamin A/C gene as causes of dilated cardiomyopathy and conduction-system disease. *N Engl J Med*. 1999;341:1715–1724. [Context Link]

3.Parks SB, Kushner JD, Nauman D, Burgess D, Ludwigsen S, Peterson A, Li D, Jakobs P, Litt M, Porter CB, Rahko PS, Hershberger RE. Lamin A/C mutation analysis in a cohort of 324 unrelated patients with idiopathic or familial dilated cardiomyopathy. *Am Heart J*. 2008;156:161–169. [Context Link]

4.Taylor MRG, Fain PR, Sinagra G, Robinson ML, Robertson AD, Carniel E, Di Lenarda A, Bohlmeyer TJ, Ferguson DA, Brodsky GL, Boucek MM, Lascor J, Moss AC, Li WLP, Stetler GL, Muntoni F, Bristow MR, Mestroni L. Natural history of dilated cardiomyopathy due to lamin A/C gene mutations. *J Am Coll Cardiol*. 2003;4:771–780. [Context Link]

5.Pasotti M, Klersy C, Pilotto A, Marziliano N, Rapezzi C, Serio A, Mannarino S, Gambarin F, Favalli V, Grasso M, Agozzino M, Campana C, Gavazzi A, Febo O, Marini M, Landolina M, Mortara A, Piccolo G, Vigano M, Tavazzi L, Arbustini E. Long-term outcome and risk stratification in dilated cardiolaminopathies. *J Am Coll Cardiol*. 2008;52:1250–1260. [Context Link]

6.Sullivan T, Escalante-Alcade D, Bhatt H, Anver M, Bhat N, Nagashima K, Stewart CL, Burke B. Loss of A-type lamin expression compromises nuclear envelope integrity leading to muscular dystrophy. *J Cell Biol*. 1999;147:913-919. [Context Link]

7.Nikolova V, Leimena C, McMahon AC, Tan JC, Chandar S, Jogia D, Kesteven S, Michalicek J, Otway R, Verheyen F, Rainer S, Stewart CL, Martin D, Feneley MP, Fatkin D. Defects in nuclear structure and function promote dilated cardiomyopathy in lamin A/C-deficient mice. *J Clin Invest*. 2004;113:357-369. [Context Link]

8.Wolf CM, Wang L, Alcalai R, Pizard A, Burgon PG, Ahmad F, Sherwood M, Branco DM, Wakimoto H, Fishman GI, See V, Stewart CL, Conner DA, Berul CI, Seidman CE, Seidman JG. Lamin A/C haploinsufficiency causes dilated cardiomyopathy and apoptosis-triggered cardiac conduction system disease. *J Mol Cell Cardiol*. 2008;44:293-303. [Context Link]

9.Lammerding J, Schulze PC, Takahashi T, Kozlov S, Sullivan T, Kamm RD, Stewart CL, Lee RT. Lamin A/C deficiency causes defective nuclear mechanics and mechanotransduction. *J Clin Invest*. 2004;113:370-378. [Context Link]

10.Lammerding J, Fong LG, Ji JY, Reue K, Stewart CL, Young SG, Lee RT. Lamins A and C but not lamin B1 regulate nuclear mechanics. *J Biol Chem*. 2006;35:25768-25780. [Context Link]

11.Hutchison CJ, Alvarez-Reyes M, Vaughan OA. Lamins in disease: why do ubiquitously expressed nuclear envelope proteins give rise to tissue-specific disease phenotypes? *J Cell Sci*. 2001;114:9-19. [Context Link]

12.Burke B, Stewart CL. Life at the edge: the nuclear envelope and human disease. *Nat Rev Mol Cell Biol*. 2002;3:575-585. [Context Link]

13.Sun M, Chen M, Dawood F, Zurawska U, Li JY, Parker T, Kassiri Z, Kirshenbaum LA, Arnold M, Khokha R, Liu PP. Tumor necrosis factor-[alpha] mediates cardiac remodelling and ventricular dysfunction after pressure overload state. *Circulation*. 2007;115:1398-1407. [Context Link]

14.Packer M, Bristow MR, Cohn JN, et al. The effect of carvedilol on morbidity and mortality in patients with chronic heart failure. *N Engl J Med*. 1996;334:1349-1355. [Context Link]

15.Fernando P, Bonen A, Hoffman-Goetz L. Predicting submaximal oxygen consumption during treadmill running in mice. *Can J Physiol Pharmacol*. 1993;71:854-857. [Context Link]

16.Nakamura A, Yoshida K, Takeda S, Dohi N, Ikeda S. Progression of dystrophic features and activation of mitogen-activated protein kinases and calcineurin by physical exercise in hearts of *mdx* mice. *FEBS Lett*. 2002;520:18-24. [Context Link]

17.Nishio R, Shioi T, Sasayama S, Matsumori A. Carvedilol increases the production of interleukin-12 and interferon-[gamma] and improves the survival of mice infected with the encephalomyocarditis virus. *J Am Coll Cardiol*. 2003;41:340-345. [Context Link]

18.Suleymanian MA, Baumgarten CM. Osmotic gradient-induced water permeation across the sarcolemma of rabbit ventricular myocytes. *J Gen Physiol*. 1996;107:503-514. [Context Link]

19.Seul M, O'Gorman L, Sammon M. Analysis of point patterns. In: Seul M, O'Gorman L, Sammon M, eds. *Practical Algorithms for Image Analysis*. Cambridge, United Kingdom: Cambridge University Press; 2000:221-245. [Context Link]

20.Du XJ, Gao XM, Wang B, Jennings GL, Woodcock EA, Dart AM. Age-dependent cardiomyopathy and heart failure phenotype in mice overexpressing [beta]$_2$-adrenergic receptors in the heart. *Cardiovasc Res*. 2000;48:448-454. [Context Link]

21.Roos KP. Length, width, and volume changes in osmotically stressed myocytes. *Am J Physiol Heart Circ Physiol*. 1986;251:H1373-H1378. [Context Link]

22.Wang Y. Mitogen-activated protein kinases in heart development and diseases. *Circulation*. 2007;116:1413-1423. [Context Link]

23.Muchir A, Pavlidis P, Decostre V, Herron AJ, Arimura T, Bonne G, Worman HJ. Activation of MAPK pathways links *LMNA* mutations to cardiomyopathy in Emery-Dreifuss muscular dystrophy. *J Clin Invest*. 2007;117:1282–1293. [Context Link]

24.Arimura T, Helbling-Leclerc A, Massart C, Varnous S, Niel F, Lacene E, Fromes Y, Toussaint M, Mura AM, Keller DI, Amthor H, Isnard R, Malissen M, Schwartz K, Bonne G. Mouse model carrying H222P-*Lmna* mutation develops muscular dystrophy and dilated cardiomyopathy similar to human striated muscle laminopathies. *Hum Mol Genet*. 2005;14:155–169. [Context Link]

25.Mounkes LC, Kozlov SV, Rottman JN, Stewart CL. Expression of an *LMNA-N195K* variant of A-type lamins results in cardiac conduction defects and death in mice. *Hum Mol Genet*. 2005;14:2167–2180. [Context Link]

26.Wang Y, Herron AJ, Worman HJ. Pathology and nuclear abnormalities in hearts of transgenic mice expressing M371K lamin A encoded by an *LMNA* mutation causing Emery-Dreifuss muscular dystrophy. *Hum Mol Genet*. 2006;15:2479–2489. [Context Link]

27.Konhilas JP, Leinwand LA. The effects of biological sex and diet on the development of heart failure. *Circulation*. 2007;116:2747–2759. [Context Link]

28.Warren DT, Zhang Q, Weissberg PL, Shanahan CM. Nesprins: intracellular scaffolds that maintain cell architecture and coordinate cell function? *Expert Rev Mol Med*. 2005;7:1–14. [Context Link]

29.Lee JSH, Hale CM, Panorchan P, Khatau SB, George JP, Tseng Y, Stewart CL, Hodzic D, Wirtz D. Nuclear lamin A/C deficiency induces defects in cell mechanics, polarization, and migration. *Biophys J*. 2007;93:2542–2552. [Context Link]

30.Pina IL, Apstein CS, Balady GJ, Belardinelli R, Chaitman BR, Duscha BD, Fletcher BJ, Fleg JL, Myers JN, Sullivan MJ. Exercise and heart failure. A statement from the American Heart Association Committee on exercise, rehabilitation, and prevention. *Circulation*. 2003;107:1210–1225. [Context Link]

31.Milner DJ, Taffet GE, Wang X, Pham T, Tamura T, Hartley C, Gerdes AM, Capetanaki Y. The absence of desmin leads to cardiomyocyte hypertrophy and cardiac dilation with compromised systolic function. *J Mol Cell Cardiol*. 1999;31:2063–2076. [Context Link]

32.Han R, Bansal D, Miyake K, Muniz VP, Weiss RM, McNeill PL, Campbell KP. Dysferlin-mediated membrane repair protects the heart from stress-induced left ventricular injury. *J Clin Invest*. 2007;117:1805–1813. [Context Link]

33.Cheng J, Kamiya K, Kodama I. Carvedilol: molecular and cellular basis for its multifaceted therapeutic potential. *Cardiovasc Drug Rev*. 2001;19:152–171. [Context Link]

34.Caron M, Auclair M, Donadille B, et al. Human lipodystrophies linked to mutations in A-type lamins and to HIV protease inhibitor therapy are both associated with prelamin A accumulation, oxidative stress and premature cellular senescence. *Cell Death Differ*. 2007;14:1759–1767. [Context Link]

35.Charniot JC, Bonnefont-Rousselot D, Marchand C, Zerhouni K, Vignat N, Peynet J, Plotkine M, Legrand A, Artigou JY. Oxidative stress implication in a new phenotype of amyotrophic quadricipital syndrome with cardiac involvement due to lamin A/C mutation. *Free Radic Res*. 2007;41:424–431. [Context Link]

Novelty and Significance

What Is Known?

* Mutations in the *LMNA* gene, which encodes the nuclear lamina proteins lamin A and lamin C, are the most common cause of familial DCM.

* *Lmna*$^{+/-}$ mice develop adult-onset DCM.

* Lamin A/C deficiency in humans and in mice alters nuclear morphology and nuclear mechanical properties.

What New Information Does This Article Contribute?

* In vivo evidence that mechanical stress-induced apoptosis is not a primary determinant of DCM in *Lmna*$^{+/-}$ mice.

* Support for a model in which changes in cytoskeletal properties caused by loss of normal nuclear anchoring impair force transmission in *Lmna*$^{+/-}$ cardiomyocytes.

* First demonstration that regular moderate exercise training and early administration of carvedilol can modify disease progression in lamin A/C-deficient hearts.

LMNA mutations are the most common cause of familial dilated cardiomyopathy (DCM), but the mechanisms linking nuclear defects to contractile dysfunction are unresolved. Lamin A/C-deficient nuclei have altered cytoarchitecture and structural properties, and, hence, mechanical stress-induced apoptosis has been widely proposed as a key factor in DCM pathogenesis. We evaluated this "structural hypothesis" in heterozygous *Lmna* knockout (*Lmna*$^{+/-}$) mice and found that despite cardiomyocyte nuclear abnormalities, young *Lmna*$^{+/-}$ mice subjected to exercise training or thoracic aortic constriction did not have increased vulnerability to apoptosis or accelerated DCM. In addition to nuclear defects, *Lmna*$^{+/-}$ cardiomyocytes show disorganization of perinuclear desmin and exaggerated responses to hypo-osmotic stress. These observations support an alternative disease model in which loss of nuclear-cytoskeletal connections destabilizes the cytoskeletal scaffolding and impairs force transmission in cardiomyocytes. Early recognition of individuals at risk in families with *LMNA* mutations provides an opportunity for intervention to prevent DCM, but this has not been investigated previously. Here we find, for the first time, that regular moderate exercise and administration of carvedilol to young male *Lmna*$^{+/-}$ mice can attenuate the development of DCM. These findings have implications for exercise recommendations and provide a basis for clinical trials in presymptomatic genotype-positive family members.

Key Words: familial dilated cardiomyopathy; lamin A/C; mechanical stress; exercise; carvedilol

---

IMAGE GALLERY

Select All Export Selected to PowerPoint

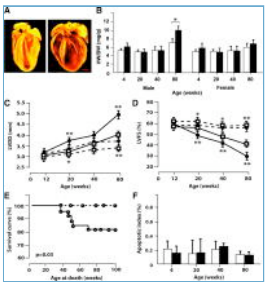

Figure 1

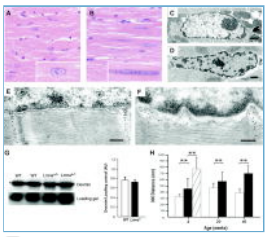

Figure 2

Table 1. Functional Studies of Ventricular Cardiomyocytes

	Male		Female	
	WT	*Lmna*$^{+/-}$	WT	*Lmna*$^{+/-}$
Myocyte length (μm)	121±10	126±8	116±8	122±5
Myocyte width (μm)	28±4	27±3	26±3	24±2
Sarcomere length (μm)	1.61±0.03	1.62±0.04	1.57±0.06	1.60±0.05
Shortening (%)	4.4±1.2	4.2±1.6	4.9±1.7	3.8±1.1
Time to peak shortening (ms)	67±8	66±16	65±5	60±7
Time to 50% relaxation (ms)	70±18	64±22	62±12	64±12
Baseline Ca^{2+} transient	0.80±0.07	0.78±0.08	NA	0.76±0.06
Peak transient amplitude	0.23±0.03	0.25±0.08	NA	0.24±0.04
Time to peak amplitude (ms)	48±10	41±8	NA	34±8
Time to 50% decay (ms)	120±38	144±29	NA	164±29

Ventricular cardiomyocytes (n=80–84 each group) were isolated from WT (n=17, 11 male) and *Lmna*$^{+/-}$ (n=17, 10 male) mice aged 40 weeks. Contractile function was assessed using edge detection. Cells were loaded with the Ca^{2+}-sensitive fluorescent dye Indo-1/AM, and intracellular [Ca^{2+}] was measured as the change in the 405:485 nm emission ratio. Values are reported as relative change in fluorescence ratio units following subtraction of background values. NA indicates not available.

Table 1

Table 2. Osmotic Studies in Ventricular Cardiomyocytes

	12 Weeks		40 Weeks	
	WT	*Lmna*$^{+/-}$	WT	*Lmna*$^{+/-}$
No. cells	120	120	79	80
Baseline				
Length (μm)	122.3±11.4	120.7±7.3	137.4±6.0	141.9±4.3
Width (μm)	21.4±1.6	20.3±1.6	26.4±0.9	25.6±1.3
1T				
Length (μm)	121.8±12.3	120.1±8.2	132.0±9.0	137.6±9.1
Width (μm)	21.5±1.7	20.0±1.9	26.8±1.5	26.5±2.2
0.5T				
Length (μm)	124.1±13.1	122.9±8.9	133.8±8.3	138.9±8.6
Width (μm)	23.6±1.8	24.4±2.0	29.9±0.7	30.6±1.4
1T (washout)				
Length (μm)	121.9±12.1	120.4±8.4	128.9±12.8	133.0±13.0
Width (μm)	21.3±1.8	20.8±2.2	27.0±1.3	26.8±1.9
Change (baseline −0.5T)				
Length (%)	1.4±1.4	1.8±2.3	2.5±4.0	2.0±3.5
Width (%)	10.4±0.8	20.2±1.7*	13.4±1.6	19.8±0.7*

Ventricular cardiomyocytes were isolated from 12- and 40-week-old male WT and *Lmna*$^{+/-}$ mice (n=4–6 each group) and placed in basic Tyrode solution. Cell dimensions were measured at baseline and 8 minutes after sequential bathing in isotonic (1T) and hypotonic (0.5T) Tyrode solution. *P<0.05 vs WT (Student *t* test).

Table 2

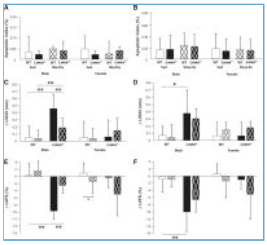

Figure 3

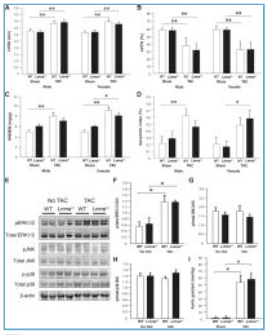

Figure 4

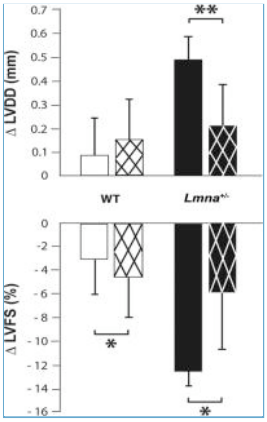

Figure 5

Non-standard Abbreviations and Acronyms	
Ab	antibody
CD	conduction system disease
DCM	dilated cardiomyopathy
ERK	extracellular signal-regulated kinase
LV	left ventricular
LVDD	left ventricular end-diastolic diameter
LVFS	left ventricular fractional shortening
MAPK	mitogen-activated protein kinase
TAC	thoracic aortic constriction
WT	wild type

Table. Non-standard ...

Back to Top